Asian Journal of Chemistry; Vol. 33, No. 12 (2021), 2934-2942

ASIAN JOURNAL OF CHEMISTRY

https://doi.org/10.14233/ajchem.2021.23397

Removal of Some Heavy Metals [Pb(II), Cd(II), Zn(II)] in Polluted Waters using Acid-Functionalized MCM-41 Mesoporous Materials: Adsorption Isotherm and Kinetic Studies

JAYARANGARAO PRATHIPATI[1,*] and PAUL DOUGLAS SANASI[2]

[1]Department of Chemistry, Baba Institute of Technology & Sciences (BITS), Visakhapatnam-530041, India
[2]Department of Engineering Chemistry, AU College of Engineering (A), Andhra University, Visakhapatnam-530003, India

*Corresponding author: E-mail: jayarangarao1@gmail.com

Received: 2 July 2021; *Accepted*: 17 August 2021; *Published online*: 6 December 2021; AJC-20583

Acid functionalized mesoporous silica materials like sulphonic acid (SO_3HMCM-41) and phosphotungstic acid (PWMCM-41) were synthesized by a simple co-precipitation method. These materials were characterized using XRD, SEM-EDS, FT-IR, BET surface area techniques. The mesoporosity was retained even after acid functionalization into MCM-41. There was a significant fall in the surface area (S_{BET}, $m^2\ g^{-1}$), on incorporation of sulphonic acid (-SO_3H) and phosphorous, tungsten atoms into the MCM-41 material. SO_3HMCM-41 was found to be more acidic than PWMCM-41 and MCM-41. Their performance was evaluated by conducting experiments on the removal of heavy metals like Pb(II), Cd(II), Zn(II) present in industrial wastewaters, with atomic absorption spectrophotometer (AAS). The required experimental factors were analyzed and it was observed that the removal of metals was more efficient with the acid-functionalized materials than with MCM-41. Freundlich adsorption isotherm and pseudo-first order kinetics have confirmed the validity of the results.

Keywords: Mesoporous silica, Wastewater treatment, Toxic metals.

INTRODUCTION

Rapid commercialization of industrial sector has led to the release of hazardous pollutants into the environment [1]. In particular, the unplanned discharge of some toxic metals into the natural waters has produced an inevitable environmental issue around the globe [2]. Many of these heavy metals are hesitant to be degraded biologically and resistant to convert into less harmful products [3]. Effluents of various industries such as mining, metal plating, manufacturing of radiators, alloys, storage cells contains mainly the heavy metal contaminants [4]. In this regard, to reduce the effect of these toxic materials on the environment, wastewater treatment guidelines have been established by United states environmental protection agency (USPEPA), which mainly focus on the maximum threshold limits of the toxic materials in the effluent waters [5]. As shown in Table-1, some of the maximum contaminated levels (MCL) of few heavy toxic metals have been represented [6].

Various methods involved in the treatment of these heavy metals from industrial wastewaters, *viz.* precipitation, membrane filtration, ion exchange, adsorption and co-precipitation/adsorption [7]. In these methods, adsorption was found to be the most efficient technique in removing the toxic metal pollutants [8]. Apart from the extensive usage of activated carbon as an efficient adsorbent, which was observed to be a costly process, several alternative economical methods have been reported for the removal of heavy metals from the contaminated waters [8]. In such route, several researchers have investigated the usage of low cost agricultural waste byproducts such as sugarcane bagasse [9-13], rice husk [14-18], sawdust [19-21], coconut husk [22], oil palm shell [23], neem bark [24], *etc.* for removing heavy metals from wastewaters. Even though these bio-adsorbentsg1 were effective in eradicating heavy metal pollutants, many of these were found to be less effective in removing metal ions present in trace limits in the wastewaters [24,25].

As an alternative, mesoporous silica was another efficient adsorbent identified by the researchers to eradicate the hazardous toxic metals, even in trace levels, from wastewaters [26]. Mesoporous silica is a highly ordered material with a regular two-dimensional hexagonal array of channels [27]. Due to high specific surface area and narrow pore size (2-10 nm), it was

TABLE-1
TOXIC EFFECTS OF FEW HEAVY METALS WITH RESPECT TO THEIR TLV [Ref. 6]

Heavy metal	Toxic effects	MCL (ppm)
Lead	Attacks fetal brain, kidneys, circulatory system and nervous system	0.006
Cadmium	Kidney and renal disorders	0.010
Zinc	Depression, lethargy, neurological signs and disorder in nervous system	0.800
Chromium	Headache, diarrhoea, nausea, vomiting, carcinogen	0.050
Arsenic	Skin infection, visceral cancers, vascular disease	0.050

reported to be effective in Cd(II) removal from wastewaters [28]. The material was also coupled with organic functional groups like carboxylic acid, sulfonic acid and amine-carbonyls and these modified forms possess enhanced catalytic properties [28]. Polyaniline/polypyrrole/hexagonal type mesoporous silica have been synthesized and analyzed for heavy metal removal of 99.2% at an optimal pH of around 8.0 [29]. SBA-15 tailored nano-porous silica was synthesized by functionalizing it with ethylenediamine, in which the material has shown a greater removal efficacy of few metal ions (98%) at pH higher than 4.5 [30]. These materials possess definite pore size, high specific surface area and good adsorption properties [31]. Compared to mesoporous MCM-41 material, its modified forms have been reported to be efficient in playing the role of adsorbents [32]. Thiol-functionalized Co-Fe_2O_4 magnetic mesoporous silica composite was synthesized using modified Stöber method and the material's adsorption capacity was investigated for the removal of Hg^{2+} ions from the aqueous solutions [33,34].

On the basis of these inputs and identifying the importance of mesoporous materials as efficient adsorbents, the present research work was designed to remove some heavy metals like Pb(II), Cd(II) and Zn(II) from their experimental solutions using these mesoporous materials. Acid functionalized MCM-41 materials like sulphonic acid MCM-41 (SO_3HMCM-41), phosphotungstic acid MCM-41 (PWMCM-41) were synthesized using facile co-precipitation method along with its parent template MCM-41. The materials were characterized using XRD, SEM-EDS, FTIR, BET surface area techniques and their adsorption capacity has been analyzed by examining the supporting factors like role of pH, contact time, catalyst weight and concentration of the metal ion solution. Further, the rate of adsorption was investigated by applying Freundlich adsorption model and the pseudo-first order kinetic profile was analyzed in order to authenticate the experimental results with the adsorption and kinetic studies, respectively.

EXPERIMENTAL

Cetyltrimethylammoniumbromide (CTAB) and tetraethyl orthosilicate (TEOS) were procured from Sigma-Aldrich, Ammonia (NH_3, AR grade) and ethyl alcohol (EtOH, AR grade) and sulphuric acid (98%), phosphotungstic acid ($H_3PW_{12}O_{40}$) were obtained from SRL laboratories, India. Lead(II) chloride, cadmium(II) chloride and zinc(II) chloride were used as the metal ion solutions, to study the removal of the respective metal ion, Pb(II), Cd(II) and Zn(II) from the aqueous solutions. Experimental solutions were prepared using double distilled water.

Synthesis of acid functionalized MCM-41 materials: In order to synthesize these transformed MCM-41 materials, its parent template MCM-41 was synthesized using a simple co-precipitation method using appropriate proportions of the silica precursor, TEOS and the surfactant, CTAB.

Sulfonic acid functionalized MCM-41 (SO_3HMCM-41): In this step, 0.5 N conc. H_2SO_4 (25 mL) was taken in a beaker and to this, 1.5 g of calcined MCM-41 was dispersed. The contents in the beaker were kept under ultrasonication for 2-3 h near the room temperature. The resultant mixture was kept under heating at around 70-80 ºC for 30-40 min. The resultant slurry obtained was dried near 110-120 ºC for 5-6 h.

Phosphotungstic acid functionalized MCM-41 (PWMCM-41): To a clear methanolic solution, 0.5 of phosphotunstic acid was added and then 1.5 g of calcined MCM-41 was dispersed. The contents were kept under ultrasonication for 18-20 h near the room temperature. The gel obtained was evaporated and dried near 110-120 ºC for 30-40 min.

Determination of acid strength: The surface acidity of the mesoporous materials was determined by ion exchange method through a simple acid base titration. To a series of three separate beakers filled with 50 mL of 0.1 N KCl solution, 0.1 of each mesoporous materials was dispersed. The solution has the ability to exchange the H^+ ions on the surface of the materials. The suspensions were boiled at around 100 ºC for about 30-40 min. The resultant suspensions were centrifuges (5000 rpm), filtered and the solid residue was separated. The supernatant liquid was titrated with a known concentration of NaOH, which was earlier standardized with a standard solution of oxalic acid. Finally, the acidity on the surface of the materials was obtained as 0.002 N, 0.109 N and 0.041 N in MCM-41, sulphonic acid and phosphotungtic acid MCM-41, respectively. These results indicate the existence of higher acidic nature on the surface of SO_3HMCM-41 material compared to the other materials and it was anticipated that the material could display pronounced catalytic properties. Therefore, the catalytic ability of the materials was examined by conducting adsorption process towards the removal of some selected hazardous heavy metals in wastewaters.

Detection method: The synthesized acid functionalized MCM-41 materials along with its parent template (MCM-41) have been characterized using X-ray diffractometer in the range of 2θ = 5-10º by step scanning on the Rigaku D/MAX-2500 diffractometer (Rigaku Co., Japan) with Cu$K\alpha$-radiation (λ = 0.15406 nm) operated at 40 kV and 100 mA. SEM images of the samples were taken using a Philips XL 30 ESEM scanning electron microscope (FEI-Philips Company, Hillsboro, USA). Quantachrome Nova 2000e surface area and pore size analyzer

has been employed for the surface area measurements of the catalysts by nitrogen adsorption-desorption under liquid nitrogen atmosphere (77 K). Fourier transform infrared spectral (FT-IR) data was recorded from BRUKER ALPHA FT-IR with Opus 6.1 version using KBr pellets at 4500-400 cm^{-1} region. Atomic absorption spectrophotometer (AAS) (iCE FIOS, Thermo-Fischer Scientific, Focal length: 250 mm, diffraction grating: 1800 lines/mm, bandwidth variable from 0.1 to 2.0 mm).

RESULTS AND DISCUSSION

XRD study: Powder X-ray diffraction patterns of MCM-41, SO_3HMCM-41 and PWMCM-41 are shown in Fig. 1. The diffraction peaks corresponding to d_{100}, d_{110} and d_{200} planes have occurred in the 2θ range of 2-10º, where the peaks represent the hexagonal moiety in the MCM-41 [35]. These peaks also designate the crystallographic ordering in the mesoporous materials. In the synthesized acid functionalized MCM-41 materials, a low angle diffraction peak was observed (d_{100}) near 2θ of 2-3º [35]. Furthermore, the peak intensity has decreased from sulphonic acid MCM-41 to phosphotungstic acid MCM-41 material and it indicates the coupling of the acid functional groups into the matrix of MCM-41 material.

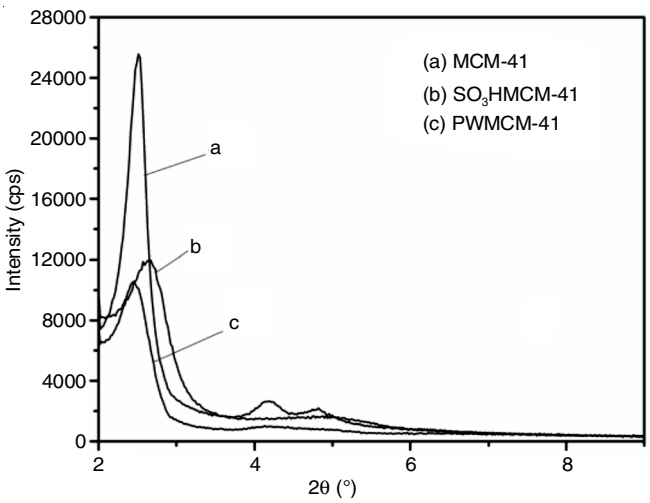

Fig. 1. XRD spectra of the mesoporous materials

SEM-EDS studies: The SEM and EDS images of MCM-41, SO_3HMCM-41 and PWMCM-41 are shown in Fig. 2. As observed from the SEM images of the materials, the morphology of the particles in all the materials was observed to be spherical in the nature. Further, there was no appreciable change in the morphology in the acid functionalized MCM-41 materials, when compared with the MCM-41 material. The presence of phosphorus, tungsten and sulphur atoms in the acid functionalized MCM-41 materials was clearly observed in the EDS spectra of the materials, along with the presence of characteristic Si, O and C atoms.

N_2 adsorption-desorption studies: The specific surface area (SSA) of the mesoporous materials were evaluated through BET (Brunauer-Emmett-Teller) method and obtained over the range of 600 to 1000 $m^2\ g^{-1}$. The SSA of the functionalized MCM-41 materials has reduced by introducing the acid functional groups to the framework. Typical type-IV adsorption isotherm was observed as represented in Fig. 3, indicating the formation of mesoporous nature in the acid functionalized materials along with its parent template, MCM-41 [36]. Furthermore, using multipoint BET isotherms adopted from BJH method, the pore volume and pore size were calculated and presented in Table-2. There was significant fall in both the parameters on functionalizing with acid groups into MCM-41, which could be attributed to the occupancy of some of the pores by acid groups.

TABLE-2
TEXTURAL PROPERTIES OF ACID FUNCTIONALIZED MCM-41 MATERIALS

Material	S_{BET} ($m^2\ g^{-1}$)	Pore size (Å)	Pore volume (cc g^{-1})
MCM-41	1018.7	16.9	0.23
SO_3HMCM-41	857.5	16.3	0.17
PWMCM-41	729.5	15.7	0.16

FTIR studies: The FT-IR spectra of the synthesized mesoporous materials is shown in Fig. 4. A characteristic band appears at 1644 cm^{-1} in the spectrum of MCM-41 due to the bending vibrations of the surface adsorbed water molecules [37]. The absorption bands at 1073 and 1229 cm^{-1} were formed corresponding to the stretching vibrations (asymmetric) of Si-O-Si bonds. Near 965 cm^{-1}, a band corresponding to Si-OH stretching vibration was observed [38]. The absorption bands in the range of 795-450 cm^{-1} region corresponds to the bending vibrations of Si-O-Si bonds and the band near 795 cm^{-1} particularly represents the existence of free silica in all the materials [39]. SO_3HMCM-41 exhibits the additional peaks at 1169 and 574 cm^{-1} analogous to the sulfonic acid group. The S-O stretching vibrations of the -SO_3H group was obtained in the range of 1200-1000 cm^{-1}. Due to the overlapping of these peaks with the stretching absorption peaks of Si-O-Si bonds (1130 to 1000 cm^{-1}) and with Si-CH_2-R bonds (1250 to 1200 cm^{-1}), the above peaks were not considered.

Furthermore, the non-condensed Si-OH stretching vibrations were observed near 958 cm^{-1} in all the materials. The bending vibrations of the adsorbed water molecules was observed near 1628 cm^{-1} (high intense). Four main absorption peaks observed for phosphotungstic acid at 1081 cm^{-1} (P–O_a), 983 cm^{-1} (W-O_d), 893 cm^{-1} (W–O_b–W) and 800 cm^{-1} (W–O_c–W), can be ascribed to asymmetric bond stretching vibrations. Absence of any shift in W-O_d band after functionalization on MCM-41 indicates that there is no fragmentation of phosphotungstic acid.

Removal of heavy metals: The sample solutions for the experimental study were prepared by using 0.1 N solutions of M^{n+} salts. The concentration of the M^{n+} ions was measured using AAS and the % removal of the metals was calculated using eqn. 1:

$$\text{Removal of metal ion (\%)} = \frac{A - B}{A} \times 100 \qquad (1)$$

where, A and B are the concentrations of the metal ion, before and after treatment with the mesoporous material under estab-

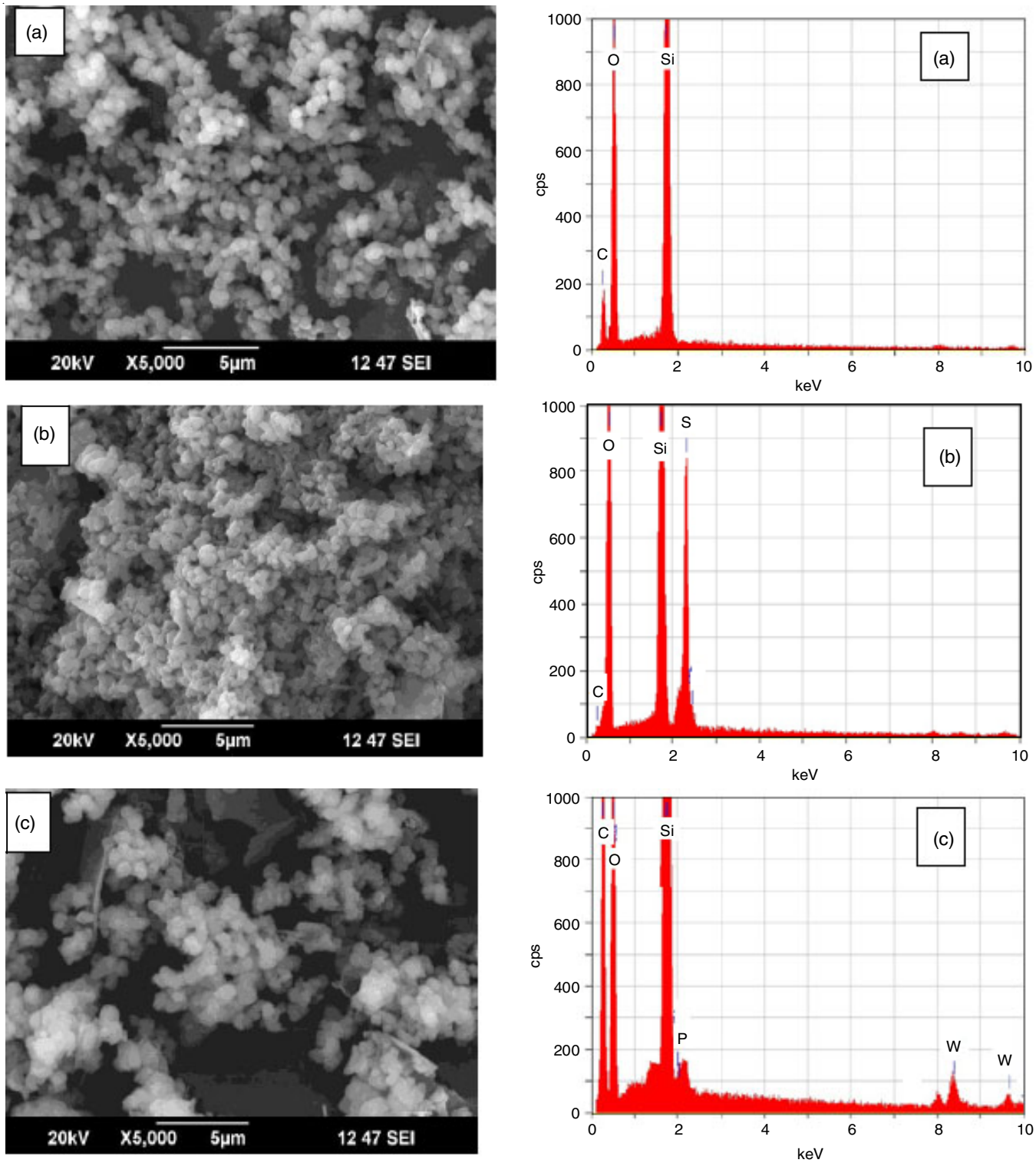

Fig. 2. SEM-EDX images of (a) MCM-41, (b) SO_3HMCM-41 and (c) PWMCM -41

lished conditions. Each experimental solution (50 mL) was taken in 250 mL beaker and a known weight of mesoporous material (mg) was added to it. The mixture was kept under magnetic stirring for a fixed time (min) and the resultant suspension was centrifuged (5000 rpm), filtered and the obtained supernatant liquid was analyzed with AAS, to find out the % removal of the respective metal ion in its solution.

Effect of pH: The effect of pH in the removal of the heavy metals play an important part of study [40]. Initially, the zeta potential (mV) of the synthesized mesoporous materials was determined, in order to understand the charge distribution their surface and the results are shown in Fig. 5. It was plotted between the zeta potential (P_{ZPC}, in mV) and pH of the sample solution under study. It was observed that the zeta potential of the

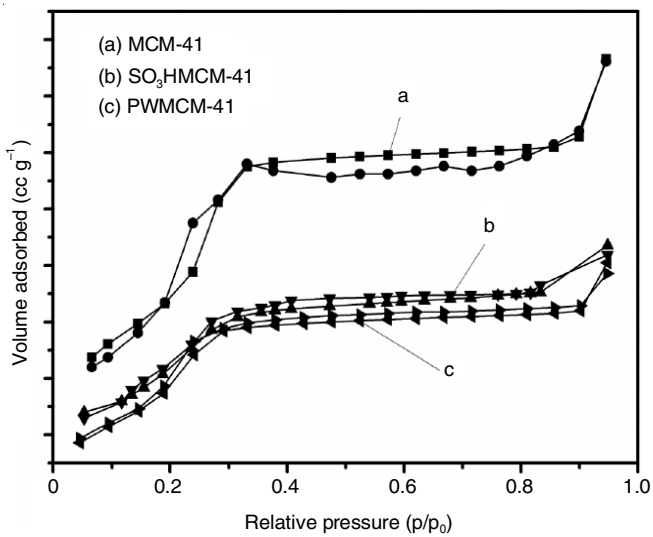

Fig. 3. Nitrogen adsorption-desorption isotherms

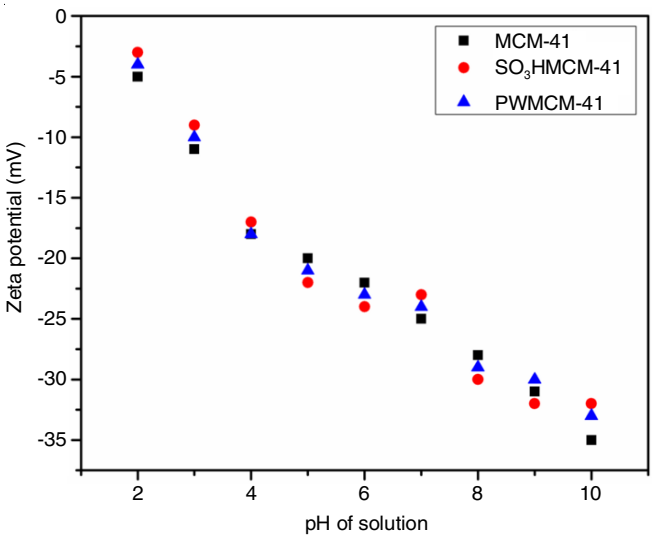

Fig. 5. Zeta potential curve of the mesoporous materials

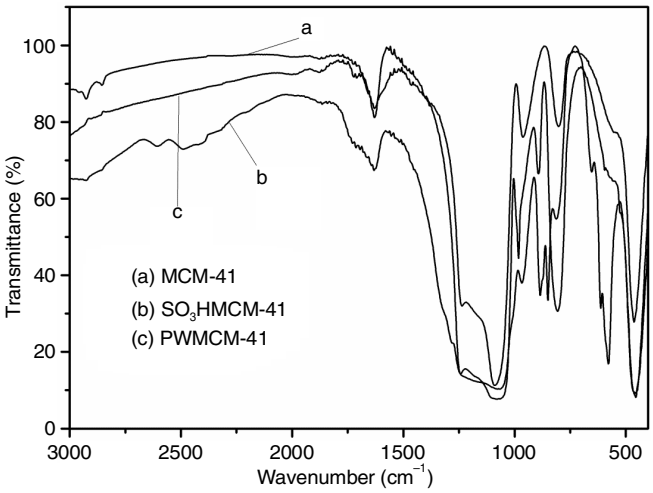

Fig. 4. FTIR spectra of (a) MCM-41, (b) SO_3HMCM-41, (c) PWMCM-41

materials has become more and more negative, with increase in pH of the solution. It signifies that the surfaces of the materials was mostly anionic, as at pH > P_{ZPC}, the surface of catalyst is cationic and at pH < P_{ZPC}, the surface is anionic in nature [41]. Hence, the catalytic performance of the mesoporous materials was active in the acidic pH range.

By varying the pH from 2.0 to 7.0 in the aqueous metal solutions and dispersing a known weight of the mesoporous materials, the experimental solutions were stirred magnetically for fixed period and the concentration of the metal ion in the solutions before and after its contact with the mesoporous materials was recorded with the AAS. From the results (Table-3), it can be observed that with increase in pH of the solution, the % removal tendency has increased up to pH 5.0. With further increase in pH, the removal tendency was observed to fall up to pH 7.0.

Hence, in these studies, it was concluded that the optimal pH for the removal of the selected metal ions with the synthesized mesoporous materials is around 5.0. Further, removal tendency has increased in acid-functionalized MCM-41 materials than with MCM-41, even though the later possess more specific area. This condition might have arrived due to the acidic nature on the SO_3HMCM-41 and PWMCM-41 materials, embedded with more number of catalytic active sites.

Effect of weight of catalyst: The next important factor, which can decide the effectiveness of a catalyst is its composition in the reaction medium [42]. Using the pH criteria and to determine the correct composition of the mesoporous materials (mg) towards the removal of the selected toxic metals, the studies were conducted and the results are shown in Table-4. It was observed that the removal of the metal has increased with increase in the catalyst weight (mg) from 5 to 15 mg/L of the solution. However, at higher weights of the catalyst, from 20 to 30 mg/L, the removal efficiency has decreased. At higher catalyst weights, the particles could agglomerate and causes less catalytic activity [42]. This leads to decreased adsorption of the metal ions on the surface of the mesoporous materials.

TABLE-3
ROLE OF pH ON THE REMOVAL (%) OF THE METAL IONS

pH	Pb(II)			Cd(II)			Zn(II)		
	MCM-41	SO_3HMCM-41	PWMCM-41	MCM-41	SO_3HMCM-41	PWMCM-41	MCM-41	SO_3HMCM-41	PWMCM-41
2.0	38	53	48	42	53	49	32	54	48
3.0	45	89	69	61	73	69	49	79	63
4.0	72	82	85	73	87	85	63	86	80
5.0	85	98	93	82	94	90	78	93	91
6.0	73	84	76	68	79	71	59	82	79
7.0	62	79	71	50	68	61	42	70	69

TABLE-4
ROLE OF CATALYST WEIGHT ON THE REMOVAL (%) OF THE METAL IONS

Catalyst weight (mg)	Pb(II)			Cd(II)			Zn(II)		
	MCM-41	SO_3HMCM-41	PWMCM-41	MCM-41	SO_3HMCM-41	PWMCM-41	MCM-41	SO_3HMCM-41	PWMCM-41
5	45	64	59	53	63	60	39	45	43
10	58	81	79	73	82	79	57	69	65
15	76	95	89	80	92	89	68	89	86
20	66	83	71	77	86	80	55	73	68
25	50	74	56	56	71	69	50	67	57
30	33	58	48	46	65	58	42	61	58

Role of contact time: In this experimentation, the pH of the testing solutions was maintained at 5.0 with 0.1 N HCl solution and 15 mg of mesoporous material was dispersed in each testing solution. The time of contact was studied by fixing the time intervals in the range of 2 to 12 min with a difference of 2 min at each trial. As displayed in Table-5, with increase in contact time of the metal ion solutions with the mesoporous materials, the % removal of the metal ions has increased up to 10 min of contact time. However, at 12 min of contact time, the % removal of the metal ions has decreased with all the mesoporous materials. Hence, the results revealed that the effective removal of the metal ions was observed at 10 min of contact time with the synthesized mesoporous materials.

Action of concentration of metal(II) ion: The rate of adsorption of metal ions (adsorbate) on the surface of the mesoporous materials (adsorbent) also depends on its concentration. Hence, the studies were conducted with the above established optimal factors and results are displayed in Table-6. It was observed that with increase in the concentration from 1 to 7 ppm the rate of adsorption has increased and from then the tendency has decreased by changing the concentration from 7 to 8 ppm. At higher concentrations of solute, the number of available active sites on the fixed weight of the catalyst would be less and causes less rate of adsorption [43].

From these experiments, it was observed finally that the adsorption capacity order is: SO_3HMCM-41 > PWMCM-41 > MCM-41 materials, respectively. Even though the specific surface area was more in MCM-41 (1018.7 m^2 g^{-1}), its adsorption capacity was less than that of its acid functionalized forms. These forms possess less specific surface area than MCM-41 material, but their adsorption capacity was more and further the activity was higher in SO_3HMCM-41 than PWMCM-41 material. In order to further investigate these observations, Freundlich adsorption model was applied on the results along with the pseudo-first order kinetic studies. These studies were mainly conducted to evaluate the adsorption capacity of the mesoporous materials. As from the above results, the removal tendency was observed to be more in the removal of Pb(II) ion, the forthcoming studies were conducting with same.

Adsorption isotherm: An adsorption isotherm was applied by establishing a graphical relation between the amount of

TABLE-5
ROLE OF CONTACT TIME ON THE REMOVAL (%) OF THE METAL IONS

Contact time (min)	Pb(II)			Cd(II)			Zn(II)		
	MCM-41	SO_3HMCM-41	PWMCM-41	MCM-41	SO_3HMCM-41	PWMCM-41	MCM-41	SO_3HMCM-41	PWMCM-41
2	32	45	40	28	35	32	34	43	40
4	45	54	52	43	48	43	45	58	52
6	58	69	63	58	63	60	52	68	61
8	69	75	71	69	79	75	63	75	70
10	72	89	85	73	91	85	78	89	85
12	65	63	62	60	80	73	49	71	69

TABLE-6
ROLE OF CONCENTRATION OF THE METAL IONS ON THE REMOVAL (%) OF THE METAL IONS

Metal conc. (ppm)	Pb(II)			Cd(II)			Zn(II)		
	MCM-41	SO_3HMCM-41	PWMCM-41	MCM-41	SO_3HMCM-41	PWMCM-41	MCM-41	SO_3HMCM-41	PWMCM-41
1	35	45	42	42	57	51	35	43	37
2	45	58	51	52	67	61	42	56	51
3	53	63	59	63	78	68	55	78	71
4	65	78	71	68	83	79	63	83	79
5	68	85	80	72	86	81	66	89	81
6	71	89	83	76	90	80	67	90	85
7	75	93	89	77	93	88	68	92	87
8	61	80	79	61	79	68	56	79	73

Experimental factors: pH = 5.0; weight of mesoporous material = 15 mg/L; contact time = 25 min

the adsorbate getting adsorbed on the surface of the adsorbent against the equilibrium concentration of the adsorbate at a given temperature [44]. In present work, Freundlich model was adopted to confirm the results of the rate of adsorption of the metal ions on the surface of the mesoporous materials [45,46].

The model can describe the exponential distribution of active centers on the catalyst surfaces [47]. It is based on the multilayer adsorption and eqn. 2 shows its linear expression [48].

$$\ln q_e = \frac{1}{n}\ln C_e + \ln K_F \quad (2)$$

where ln q_e and ln C_e denotes the equilibrium adsorption capacity of the adsorbent (mg/g, mesoporous material) and the equilibrium concentration of the adsorbate (mg/L, metal ion), respectively. The adsorption capacity of the mesoporous materials was observed from the ln K_F (Freundlich constant) and (1/n) represents the slope indicating the surface heterogeneity of the materials.

A graph was plotted (Fig. 6) between ln q_e (*y*-axis) and ln C_e (*x*-axis), in which the factor (1/n) represents the slope and K_F indicates the intercept on the *y*-axis. It can be observed from the isotherm that the magnitude of the K_F has increased from MCM-41 (ln K_F = 0.3) to PWMCM-41 (ln K_F = 0.7) and SO_3HMCM-41 (ln K_F = 1.1) mesoporous materials respectively, with almost similar trends in their slopes. It denotes the higher adsorption capacity of SO_3HMCM-41 material than PWMCM-41, which was further better adsorbent than MCM-41 material. The results show that the acid functionalization of MCM-41 has improved the adsorption tendency of the mesoporous materials. Furthermore, the rate of adsorption has increased with increase in the concentration of the metal ion from 1 to 7 ppm progressively. With further increase in the metal concentration, the adsorption capacity was almost constant, by varying the concentration from 7 to 12 ppm.

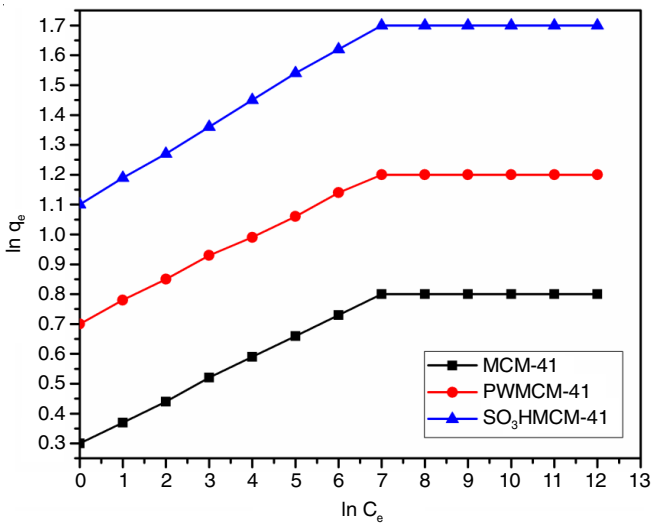

Fig. 6. Freundlich adsorption isotherm

Kinetic studies: In the phenomenon of adsorption, the study of kinetics plays an important role in understanding the rate of adsorption of the adsorbates on the surface of the adsorbent [49]. For liquid-solid phase based adsorption systems, pseudo-first order kinetic model can be applied to describe the adsorption phenomenon [50]. According to this model, the eqn. 3 describes its kinetic expression [51].

$$\frac{dq_e}{dt} = K(q_e - q_t) \quad (3)$$

The integral form is expressed as eqn. 4:

$$\log(q_e - q_t) = \log q_e - \frac{kt}{2.303} \quad (4)$$

where, q_e and q_t represents the equilibrium adsorption capacity of the adsorbent (mg/g) and the adsorption capacity (mg/g) in a time t (min), respectively. The rate constant of the pseudo first-order adsorption model was denoted by k (min^{-1}).

A graph was plotted with log (q_e-q_t) on *y*-axis and t on *x*-axis, in which log q_e denotes the intercept on *y*-axis and -k/2.303 represents the slope of the curves.

From the adsorption kinetic profile, it was observed that the intercept log q_e (Fig. 7) was more with SO_3HMCM-41 and PWMCM-41 materials, which was comparatively higher than MCM-41 material. The pseudo first-order rate constant (k, min^{-1}) was calculated and presented in Table-7. The rate constant has increased drastically on acid functionalization of MCM-41 material, in which the highest value was observed with SO_3HMCM-41 material, indicating its efficiency in the adsorption of the selected heavy metals from polluted waters.

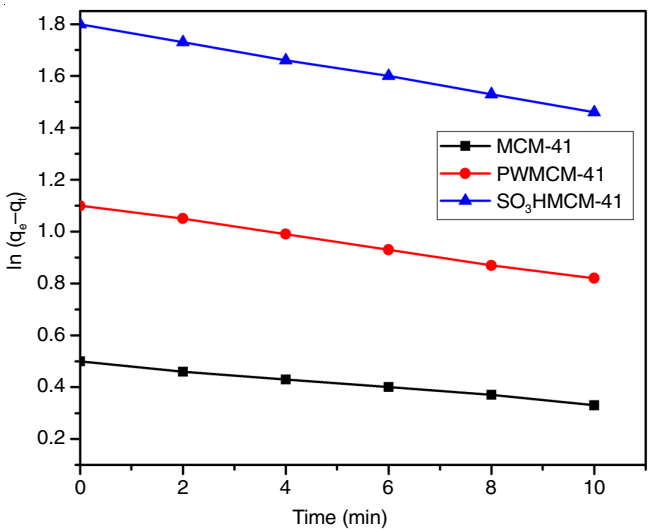

Fig. 7. Adsorption kinetic profile

TABLE-7
KINETIC PROFILE OF THE RATE OF ADSORPTION OF THE MESOPOROUS MATERIALS

Mesoporous material	Pseudo first order rate constant (k) (min^{-1})
MCM-41	2.83×10^{-3}
PWMCM-41	5.27×10^{-3}
SO_3HMCM-41	7.20×10^{-3}

Based on the above results, it was observed that the synthesized acid functionalized mesoporous silica materials were highly efficient adsorbents in eliminating the selected toxic

TABLE-8
COMPARING THE RESULTS WITH EXISTING SCIENTIFIC REPORTS

Mesoporous material	Eliminated metal ions	Removal (%) of ion [or] adsorption capacity (mmol/g)	Ref.
Nano MCM-41 (5.0 g/L)	Ni(II), Cd(II), Pb(II)	Pb(II) = 85%; Ni(II) = 30 %; Cd(II) = 50 %	[52]
Nano NH_2-MCM-41 (5.0 g/L)	Ni(II), Cd(II), Pb(II)	Pb(II) = 98 % (pH = 2.5); Ni(II) = 98 % (pH = 3.5); Cd(II) = 98 % (pH = 3.5)	
NH_2-MCM-41 + EDTA (0.1 g)	Ni(II), Cd(II)	Cd(II): 0.71 (mmol/g); Ni (II): 0.69 (mmol/g)	[53]
Graphene oxide-ordered mesoporous silica	As, Cd, Cr, Hg, Pb	As = 97.7%; Cd = 96.9%; Cr = 96 %; Hg = 98.5%; Pb = 78.7%	[54]
G-SBA-15-N-C-H G-SBA-15-NNN-E G-SBA-15-NNN-E	Ni(II), Cd(II), Pb(II), Zn(II)	Ni(II) = 47%; Cd(II) = 73%; Pb(II) = 99 % Cu(II) = 58% Zn(II) = 50 %	[26]
NH_2-SBA-15-Gn-EDTA	Cu(II)	> 94 %	[55]
NH_2-mesoporous silica	Pb(II); Cu(II); Cd(II)	Pb(II) = 880.6 mg/g; Cu (II) = 628.3 mg/g; Cd(II) = 492.4 mg/g	[56]
o-Vanillin functionalized mesoporous silica	Pb(II)	80 to 90 % adsorption capacity (155.71 mg/g)	[57]
MCM-41	Pb(II)	Pb(II) = 85%; Cd(II) = 82 %; Zn(II) = 78%	Present work
SO_3HMCM-41	Cd(II)	Pb(II) = 98%; Cd(II) = 94 %; Zn(II) = 93%	
PWMCM-41 (at 15 mg/L composition)	Zn(II)	Pb(II) = 93%; Cd(II) = 90 %; Zn(II) = 91% at metal solution pH = 5.0	

metal ions, Pb(II), Cd(II) and Zn(II) under the established experimental conditions. On comparing the results (Table-8) with other reported results, involving the removal of metal ions by using acid-functionalized mesoporous materials, it was analyzed that the SO_3HMCM-41 and PWMCM-41 materials were at par and even better adsorbents. In many of these methods, co-condensation method or grafting methods were implemented to obtain various organic functional group coupled mesoporous materials. Majority of the reported works were based on functionalization of MCM-41 with amino group, higher alkyl chain (isopropyl), *etc*. to obtain efficient adsorbents. Furthermore, these materials were playing the role of effective adsorbents in the highly acidic pH range and also with higher catalyst loads. On the other hand, the SO_3HMCM-41 and PWMCM-41 materials, synthesized through a facile co-precipitation method have eliminated the selected heavy metals to the maximum extent with a very low catalyst composition (15 mg/L) and a nominal pH range (5.0). The materials were observed to be the best adsorbents as observed the results of adsorption isotherms and kinetic studies. Hence, these materials can be an alternative for the elimination of many other toxic metal ions from wastewaters, so as to contribute for controlling the industrial wastewater pollution.

Conclusion

Acid functionalized MCM-41 materials were synthesized using a simple co-precipitation method and their role towards the adsorption and removal of some heavy metal ion pollutants like Pb(II), Cd(II), Zn(II) in wastewaters. The major outcome of the present work is the usage of moderate experimental conditions with facile adsorption technique. The synthesized acid functionalized MCM-41 materials have also shown pronounced adsorption capacity under the established conditions of pH, contact time, concentration of the metal ion solution and catalyst weight. The results were strongly supported with the Freundlich adsorption model, in which the rate of adsorption ($\ln K_F = 1.1$) was found to be more with SO_3HMCM-41 material. Similar trend was observed on applying pseudo-first order kinetics, in which the material has shown the highest rate constant (7.20×10^{-3} min^{-1}) with respect to the rate of adsorption of the selected metal ions on its surface. Therefore, the materials are novel adsorbents in removing the toxic metal ions from wastewaters using a simple adsorption technique.

ACKNOWLEDGEMENTS

The authors are thankful to the Advanced Analytical Laboratory, Andhra University, Visakhapatnam, India for providing the results of XRD, FESEM-EDS and FTIR analysis, Sophisticated Instrumentation Facility (SIF), IIT Madras, Chennai, India for providing the analysis results of BET surface area techniques.

CONFLICT OF INTEREST

The authors declare that there is no conflict of interests regarding the publication of this article.

REFERENCES

1. R.P. Schwarzenbach, B.I. Escher, K. Fenner, T.B. Hofstetter, C.A. Johnson, U. Von Gunten and B. Wehrli, *Science*, **313**, 1072 (2006); https://doi.org/10.1126/science.1127291
2. J. Yang, B. Hou, J. Wang, B. Tian, J. Bi, N. Wang, X. Li and X. Huang, *Nanomaterials*, **9**, 424 (2019); https://doi.org/10.3390/nano9030424
3. H.A. Hegazi, *HBRC J.*, **9**, 276 (2013); https://doi.org/10.1016/j.hbrcj.2013.08.004
4. K. Kadirvelu, K. Thamaraiselvi and C. Namasivayam, *Bioresour. Technol.*, **76**, 63 (2001); https://doi.org/10.1016/S0960-8524(00)00072-9
5. S. K. Gunatilake, *J. Multidiscipl. Eng. Sci. Stud.*, **1**, 12 (2015).
6. S. Babel and T.A. Kurniawan, *J. Hazard. Mater.*, **97**, 219 (2003); https://doi.org/10.1016/S0304-3894(02)00263-7
7. M.T. Amin, A.A. Alazba and U. Manzoor, *Adv. Mater. Sci. Eng.*, **2014**, 825910 (2014); https://doi.org/10.1155/2014/825910
8. S.B. Chen, Y.B. Ma, L. Chen and K. Xian, *Geochem. J.*, **44**, 233 (2010); https://doi.org/10.2343/geochemj.1.0065
9. D. Mohan and K.P. Singh, *Water Res.*, **36**, 2304 (2002); https://doi.org/10.1016/S0043-1354(01)00447-X

10. N.A. Khan, S.I. Ali and S. Ayub, *Sci. Technol.*, **6**, 13 (2001).
11. S. Ayub, S.I. Ali, N.A. Khan and R.A.K. Rao, *Environ. Prot. Control J.*, **2**, 5 (1998).
12. S. Ayub, S.I. Ali and N.A. Khan, *Pollut. Res. J.*, **2**, 233 (2001).
13. S. Ayub, S.I. Ali and N.A. Khan, *Environ. Pollut. Control J.*, **5**, 10 (2002).
14. K. Srinivasan, N. Balasubramaniam and T.V. Ramakrishna, *Indian J. Environ. Health*, **30**, 376 (1998).
15. E. Munaf and R. Zein, *Environ. Technol.*, **18**, 359 (1997); https://doi.org/10.1080/09593331808616549
16. M. Ajmal, R. Ali Khan Rao, S. Anwar, J. Ahmad and R. Ahmad, *Bioresour. Technol.*, **86**, 147 (2003); https://doi.org/10.1016/S0960-8524(02)00159-1
17. R. Suemitsu, R. Uenishi, I. Akashi and M. Nakano, *J. Appl. Polym. Sci.*, **31**, 75 (1986); https://doi.org/10.1002/app.1986.070310108
18. N.A. Khan, M.G. Shaaban and Z. Jamil, Proc. UM Research Seminar organized by Institute of Research Management and Consultancy (IPPP), University of Malaya, Kuala Lumpur (2003).
19. M. Ajmal, R.A. Khan Rao and B.A. Siddiqui, *Water Res.*, **30**, 1478 (1996); https://doi.org/10.1016/0043-1354(95)00301-0
20. K. Kadirvelu, M. Kavipriya, C. Karthika, M. Radhika, N. Vennilamani and S. Pattabhi, *Bioresour. Technol.*, **87**, 129 (2003); https://doi.org/10.1016/S0960-8524(02)00201-8
21. K. Selvi, S. Pattabhi and K. Kadirvelu, *Bioresour. Technol.*, **80**, 87 (2001); https://doi.org/10.1016/S0960-8524(01)00068-2
22. W.T. Tan, S.T. Ooi and C.K. Lee, *Environ. Technol.*, **14**, 277 (1993); https://doi.org/10.1080/09593339309385290
23. M. Anjum, R. Miandad, M. Waqas, F. Gehany and M.A. Barakat, *Arab. J. Chem.*, **12**, 4897 (2019); https://doi.org/10.1016/j.arabjc.2016.10.004
24. S. Ayub, S.I. Ali and N.A. Khan, *Environ. Pollut. Control J.*, **4**, 34 (2001).
25. V. Ravindran, M.R. Stevens, B.N. Badriyha and M. Pirbazari, *Am. Inst. Chem. Eng. J.*, **45**, 1135 (1999); https://doi.org/10.1002/aic.690450520
26. J. Aguado, J.M. Arsuaga, A. Arencibia, M. Lindo and V. Gascón, *J. Hazard. Mater.*, **163**, 213 (2009); https://doi.org/10.1016/j.jhazmat.2008.06.080
27. A.S. Zola, L.S. da Silva, A.L. Moretti, A. do Couto Fraga, E.F. Sousa-Aguiar and P.A. Arroyo, *Topic in Catalysis*, **59**, 219 (2016); https://doi.org/10.1007/s11244-015-0446-1
28. M. Nookaraju and A. Rajini, *Asian J. Chem.*, **24**, 5817 (2012).
29. H. Javadian and M. Taghavi, *Appl. Surf. Sci.*, **289**, 487 (2014); https://doi.org/10.1016/j.apsusc.2013.11.020
30. L. Hajiaghababaei, A. Badiei, M.R. Ganjali, S. Heydari, Y. Khaniani and G.M. Ziarani, *Desalination*, **266**, 182 (2011); https://doi.org/10.1016/j.desal.2010.08.024
31. M. Manyangadze, N.M.H. Chikuruwo, T.B. Narsaiah, C.S. Chakra, G. Charis, G. Danha and T.A. Mamvura, *Heliyon*, **6**, e05309 (2020); https://doi.org/10.1016/j.heliyon.2020.e05309
32. T. Kegl, A. Kosak, A. Lobnik, Z. Novaka, A. Kova Kralj and I. Ban, *J. Hazard. Mater.*, **386**, 121632 (2020); https://doi.org/10.1016/j.jhazmat.2019.121632
33. T. Kegl, I. Ban, A. Lobnik and A. Kosak, *J. Hazard. Mater.*, **378**, 120764 (2019); https://doi.org/10.1016/j.jhazmat.2019.120764
34. K. Li, L. Xie, Z. Hao and M. Xiao, *J. Dispers. Sci. Technol.*, **41**, 503 (2020); https://doi.org/10.1080/01932691.2019.1591974
35. P.T. Tanev, M. Chibwe and T.J. Pinnavaia, *Nature*, **368**, 321 (1994); https://doi.org/10.1038/368321a0
36. G. Petrini, A. Cesana, G.D. Alberti, F. Genoni, G. Leofanti, M. Padovan, G. Paparatto and P. Roffia, *Stud. Surf. Sci. Catal.*, **68**, 761 (1991); https://doi.org/10.1016/S0167-2991(08)62710-X
37. J.C.P. Broekhoff, *Stud. Surf. Sci. Catal.*, **3**, 663 (1979); https://doi.org/10.1016/S0167-2991(09)60243-3
38. A. Ghanbari-Siahkali, A. Philippou, J. Dwyer and M.W. Anderson, *Appl. Catal. A*, **192**, 57 (2000); https://doi.org/10.1016/S0926-860X(99)00333-6
39. P.A. Jalil, M.A. Al-Daous, A.-R.A. Al-Arfaj, A.M. Al-Amer, J. Beltramini and S.A.I. Barri, *Appl. Catal. A*, **207**, 159 (2001); https://doi.org/10.1016/S0926-860X(00)00670-0
40. G.Z. Kyzas and K.A. Matis, *J. Mol. Liq.*, **203**, 159 (2015); https://doi.org/10.1016/j.molliq.2015.01.004
41. R.A. Mahmud, A.N. Shafawi, K. Ahmed Ali, L.K. Putri, N.I. Md Rosli and A.R. Mohamed, *Mater. Res. Bull.*, **128**, 110876 (2020); https://doi.org/10.1016/j.materresbull.2020.110876
42. S. Ryali and P.D. Sanasi, *J. Chin. Chem. Soc.*, **65**, 1423 (2018); https://doi.org/10.1002/jccs.201800154
43. S. Mustapha, D.T. Shuaib, M.M. Ndamitso, M.B. Etsuyankpa, A. Sumaila, U.M. Mohammed and M.B. Nasirudeen, *Appl. Water Sci.*, **9**, 142 (2019); https://doi.org/10.1007/s13201-019-1021-x
44. L. Theodore and F. Ricci, Mass Transfer Operations for the Practicing Engineer; John Wiley & Sons, Inc.: Hoboken, NJ, USA (2011).
45. J.N. Putro, S.P. Santoso, S. Ismadji and Y.H. Ju, *Micropor. Mesopor. Mater.*, **246**, 166 (2017); https://doi.org/10.1016/j.micromeso.2017.03.032
46. H. Baseri and S. Tizro, *Process Saf. Environ. Prot.*, **109**, 465 (2017); https://doi.org/10.1016/j.psep.2017.04.022
47. W. Shen, S. Chen, S. Shi, X. Li, X. Zhang, W. Hu and H. Wang, *Carbohydr. Polym.*, **75**, 110 (2009); https://doi.org/10.1016/j.carbpol.2008.07.006
48. H. Freundlich, *Z. Phys. Chem.*, **57**, 385 (1906).
49. M. Matouq, N. Jildeh, M. Qtaishat, M. Hindiyeh and M.Q. Al Syouf, *J. Environ. Chem. Eng.*, **3**, 775 (2015); https://doi.org/10.1016/j.jece.2015.03.027
50. S. Çavus and G. Gurdag, *Ind. Eng. Chem. Res.*, **48**, 2652 (2016); https://doi.org/10.1021/ie801449k
51. A. M. Farhan, N. M. Salem, A. H. Al-Dujaili and A. M. Awwad, *Am. J. Environ. Eng.*, **2**, 188 (2012); https://doi.org/10.5923/j.ajee.20120206.07
52. A. Heidari, H. Younesi and Z. Mehraban, *Chem. Eng. J.*, **153**, 70 (2009); https://doi.org/10.1016/j.cej.2009.06.016
53. K.F. Lam, K.L. Yeung and G. Mckay, *Environ. Sci. Technol.*, **41**, 3329 (2007); https://doi.org/10.1021/es062370e
54. X. Wang, Y. Pei, M. Lu, X. Lu and X. Du, *J. Mater. Sci.*, **50**, 2113 (2015); https://doi.org/10.1007/s10853-014-8773-3
55. Y. Jiang, Q. Gao, H. Yu, Y. Chen and F. Deng, *Micropor. Mesopor. Mater.*, **103**, 316 (2007); https://doi.org/10.1016/j.micromeso.2007.02.024
56. Q. Yuan, N. Li, Y. Chi, W. Geng, W. Yan, Y. Zhao, X. Li and B. Dong, *J. Hazard. Mater.*, **254-255**, 157 (2013); https://doi.org/10.1016/j.jhazmat.2013.03.035
57. D.C. Culita, C.M. Simonescu, R.-E. Patescu, M. Dragne, N. Stanica and O. Oprea, *J. Solid State Chem.*, **238**, 311 (2016); https://doi.org/10.1016/j.jssc.2016.04.003